

Geophysical Characterization of the Lithology and Aquifer Recharge Dynamic of Lbrbda, Mbaku Farm Project Site, Makurdi.

¹Ochai, J S, ²Nwakonobi T U, ³Enokela O S

¹GP 701Oba Olobayo Estate, Gadumo, Lokoja

^{2,3}Department of Agricultural and Environmental Engineering
Joseph Sawuan Tarka University, Makurdi

ABSTRACT

Hydrogeological and geophysical investigations were carried out in LBRBDA's farm project site, Mbaku to establish the sustainable availability of irrigation water. Vertical electrical sounding (VES) Techniques were employed in characterising the aquifer properties, hydraulic parameters from of the farm site. The farm project site has four and five geo-electric layers, namely; Lateritic top soil, clay, sandy clay or clayey sand, sandstone or sandy clay and clay. The aquiferous unit is in third and fourth layers respectively. Depth to water table ranged from 5.2 m to 32.4 m with a mean value of 12.7 m. The aquifer resistivity ranged from 12.9 Ω m to 697.4 Ω m with thickness between 8.1 m to 37.0 m and. depth to aquifer bwtween16.2 m to 86.9 m with a mean value of 42.3m. The transmissivity ranged from 9.8052 m²/day to 1027.8834 m²/day, thus classified the groundwater potential into low, intermediate, high, and very high groundwater prospective. Low transmissivity was mostly concentrated at the northeast and southeast part of the study area corresponding to observed hydraulic conductivity with a values between 0.8601 m/day to 35.5669 m/day. However, low to moderate hydraulic conductivity were observed hence permeable and suitable for drilling tube wells. The aquifers have appreciable thickness with Low to moderate hydraulic conductivity indicating aquiferous zones which are permeable and capable of yielding appreciable groundwater for irrigation, suitable for tubewell the area characterized

Keywords: LBRBDA's farm, groundwater, aquifer characteristics, VES

Date of Submission: 13-02-2025

Date of acceptance: 27-02-2025

I. INTRODUCTION

River basins are physical systems where the input is the volume of precipitated water and the output is the volume of water drained at the outlet (Petts and Foster, 1990). The variability of the hydrological regime is controlled by several elements that characterize the hydrographic basin, such as lithology, relief, soils, and vegetation cover, also by climatic factors such as precipitation, solar radiation and evaporation (Tucci, 2002). According to Clarke *et al.* (2003), factors such as geographic location and/or altitude may contribute substantially to the results of flow regime analysis, air mass advancement and local precipitation events, among others. Prospecting groundwater in the past was based on consideration of important parameters such as overburden thickness, weathered layer resistivity, bedrock resistivity, aquifer layer resistivity and aquifer layer thickness among others (Clark,1985; Omosuyi, and Oseghale; Abiola *et al.*, 2009; Adeyemo, *et al.*, 2014; Amadi, *et al.*, 2011; Kosinski, *et al.*, 1981; Mogaji *et al.*, 2011; Olayanju *et la.*, 2011) and each parameter is considered in isolation.

Groundwater development in river basins required hydrogeological and geophysical techniques such as electrical resistivity, seismic, magnetic, electromagnetic, ground probing radar, pumping test and down-hole logging (Anomohanran, 2013). Among the geophysical methods, the geoelectric resistivity method is being used mostly for investigating the groundwater strata because of has simple instrumentation and easy field operations as well as analysis of data than other methods (Hasan *et al.*, 2018; Shah *et al.*, 2023; Wahab *et al.*, 2021). The data can be employed for identification and nature of aquifers and characterize the subsurface elements including quality of groundwater (Oldenborger *et al.*, 2007). Amiri *et al.* (2023) and Hasan *et al.* (2018) posited that resistivity data of geophysical methods could help in identifying the availability of potential groundwater repositories. A fundamental correlation can be established by integration of hydraulic parameters from resistivity data according to (Mohammed *et al.*, 2023; Niwas *et al.*, 2006; Oli *et al.*, 2022; Umoh *et al.*, 2022).

The Lower Benue River Basin (LBRB), Makurdi like any other river basins in the world has potentials for groundwater prospecting for irrigation and domestic uses. However, it has being challenged with low rainfall amount and duration and hence need to explore other water sources for irrigation purpose (Silva-Junior, 2003).

There is difficulty in getting water from the River Benue to the rich Fadama lands of Project farm for irrigation by Lower Benue River Basin Development Authority (LBRBDA).

The primary aim of this study is to explore the potentials for groundwater resources for irrigation in LBRB project farm at Mbaku. The specific objectives are; to characterize the lithology of the aquifer formation, to evaluate the recharge dynamic, to develop a geological water table/other hydrogeological maps of the study area to serve as a guide to intending farmers in siting and drilling of tubewells.

II. METHODOLOGY

2.1 Study area

The LBRBDA farm project at Mbaku Makurdi and lies between Latitude $07^{\circ} 30' 00''$ N to $08^{\circ} 00' 00''$ N and Longitude $08^{\circ} 15' 00''$ E to $08^{\circ} 50' 00''$ E (Figure 1). The Project site covers an area of 11,491,339.55 square metres (1149 Hectares) with a perimeter of 14,635.9739 metres (14.64 kilometres). The Project site was sub divided into twenty-two (22) equal blocks of approximately 52.23 hectares each (Fig. 2). It is located in Benue State which is bound in the North East by Nassarawa State, North West by Kogi state, South East by Cross River State and in the East by Enugu and Ebonyi States. Makurdi falls in the

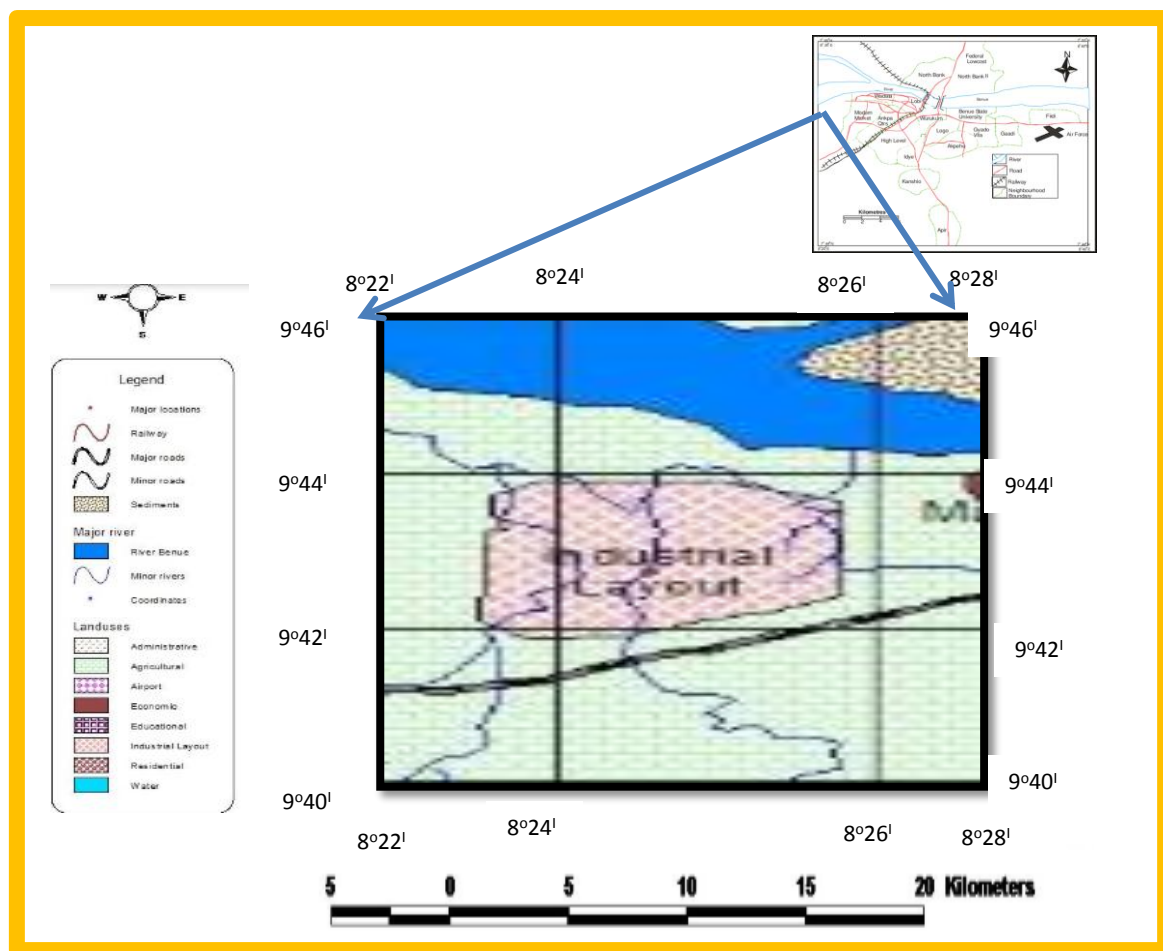


Figure 1: Makurdi Local Government Area Map Showing Study Area (Mbaku)

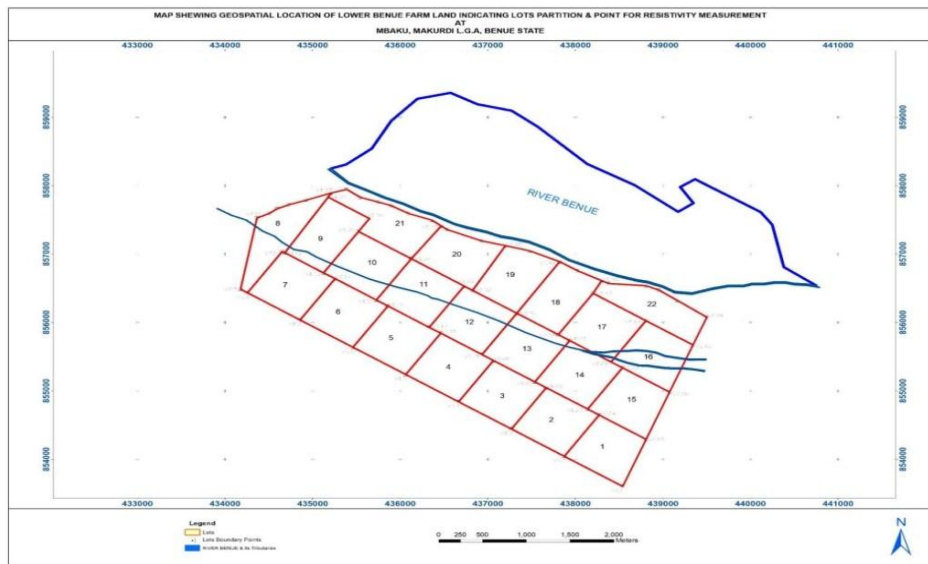


Figure 2: Sub division of the farm sites

Southern Guinea Savannah which is a transition belt between the grassland Savannah in the North and the rain forest in the South. The vegetation cover is mostly made up of giant grasses (elephant grass) and tree species like, Shear tree (*Vitellaria paradoxa*), African locust bean tree (*Parkia biglobosa*), Iron tree or African mesquite (*Prosopis africana*) – okpehe in Igala/Idoma and Gbaaaye tree in Tiv language etc. Along the banks of the river Benue are found hydromorphic soils which are fertile for several crops' cultivation. Generally, Makurdi soils vary from sandy to loamy soil in some part of the Local Government Area. Makurdi LGA has a total land area of 3,993.3 Km² (Ityavyar *et al.*, 2011). The climate is referred to as a local steppe climate. There is little rainfall throughout the year. This location is classified as BSh (i.e Hot arid steppes) by Koppen and Geiger. The average temperature here is 26.1°C. The study area falls within the southern Guinea climatic zone of Nigeria and like other parts of the country, two distinct seasons occur, these are; the dry season which lasts from November to April and the rainy season which starts in April and lasts till the end of October. The annual rainfall depth ranges from about 1,200 mm to 1,500 mm with an average depth of about 1350 mm. Wind speed at 5 Km/h, Humidity – 84%. The peak of the rainy season is usually between July and August.

2.2 Geospatial survey of LBRBDA's farmland

The main reason of the geospatial map and the partitions is to establish well distributed points for geophysical surveys (VES points) within the study area to develop the relevant hydrogeological maps. The areas and perimeters of the plots (blocks) are in square metres and metres and their equivalents in hectares and kilometres respectively. Coordinates of points at the project site were acquired using Garmin Montana 680 hand held Global Positioning System (GPS) receiver by Universal Traverse Mercator (WGS – 84 UTM) Zone 32N reference coordinates system. Resistivity measurements were performed at the corners of each plots and elevation data acquired using Garmin Montana 680. Auto CAD 2010 ArcGIS 10 software was utilized to produce the geospatial map

2.3 Geophysical survey of LBRBDA's farmland

Surface geophysical method is one of the groundwater investigation methods frequently used to prospect ground water. Geophysical Surveys were conducted using an Ohmega (Ω) Terrameter on forty - six (46) vertical electrical sensitivity (VES) established and probed points. The investigations were carried out in the Month of March which is agreeably the peak of the dry season when Static water table (SWT) is lowest in Makurdi. Schlumberger electrode configuration (Akhter *et al.*, 2016; Akintorinwa *et al.*, 2019; Anomohanran, 2015; Erram, *et al.*, 2010; Hasan *et al.*, 2022), maximum half-current electrode (AB/2) spreading range from 1m to 100 m and the half potential electrodes (MN/2) range between 0.25 m to 5 m were adopted for this study (Manu *et al.*, 2019; Mehmood *et al.*, 2020; Oyeyemi *et al.*, 2021; Sikandar *et al.*, 2010; Taha *et al.*, 2021), given the shallow depth of Tubewells. The coordinate of the centroid was determined by GPS while the linear measurement of the length of current and potential electrodes spreading were measured by tape. The Terrameter was switched ON and the current sent to the ground which in-turn gave back a resistance (R), the geometric factor (K) was calculated as in equation 1 and was used to compute the apparent resistivity (ρ_a) using equation 2. (Nwachukwu *et al.*, 2007; Subba, 2003).

$$k = \pi \left[\frac{\left(\frac{AB}{2}\right)^2 - \left(\frac{MN}{2}\right)^2}{MN} \right] \quad (1)$$

$$\rho_a = \pi \left[\frac{\left(\frac{AB}{2}\right)^2 - \left(\frac{MN}{2}\right)^2}{MN} \right] R \quad (2)$$

Where:

k is the geometric factor,

ρ_a is the apparent resistivity,

R is the resistance.

The procedure was repeated after every 0.5 m position of the current electrodes keeping the potential electrodes position constant. for maximum current electrode of 100 m. The above procedure was adopted for all the sounding points taken within the study area.

2.4 Data analysis/processing

The data set obtained from the field were processed manually and further analysed using computer software techniques in order to obtain aquifer parameters such as layer resistivity, thickness and depth. The manual techniques was done by plotting the graph of apparent resistivity (ρ_a) against half-electrode spacing (AB/2) on a logarithmic graph; the plotted graphs gave a representative curve type, number of geo-electric layers with their resistivity, thickness and depth for different sounding points. A typical manual curve procedure was used to quantitatively interpret the geophysical properties of the farm site. This information obtained from the manual processing techniques were then input into a computer software (WinResist) as input data for the computer iterative analysis based on linear filter theory according to Zohdy (1989) which gave smooth curves with individual layer resistivity, layer thickness and depth as output.

RESULTS

Figure 1 is the VES Curve at location 1 as a representative example of all the 46 points. The plot provided for the automatic generation of the aquifer thickness and depth from the relationship between the resistivity and the current electrode distances. The lower the resistivity, the higher the aquifer thickness and depth respectively according to interpreted geo-electrical layer result obtained from the plotted graphs of current electrode distance against apparent resistivity.

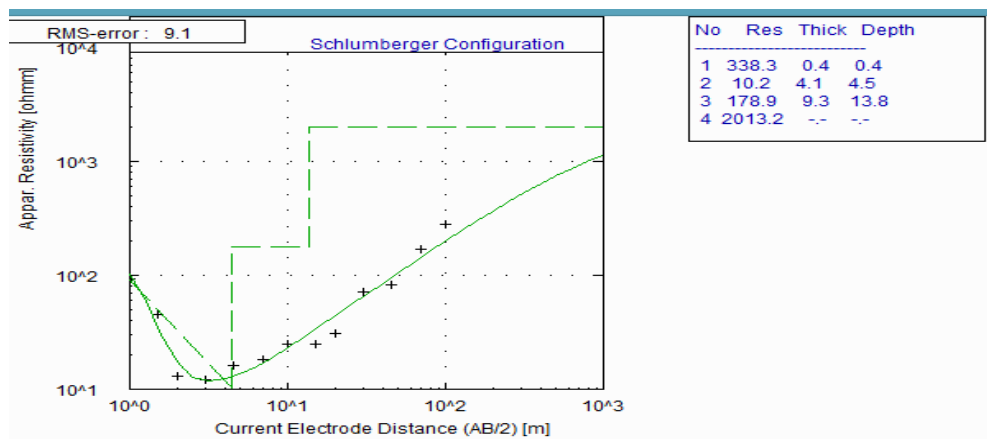


Figure 1: VES Curve at Location 1

Table 1 is the results of the geoelectrical layers; from the Table, it can be seen that the VES points having four geo-electric layers include; VES 1, 2, 4, 5, 9, 12, 14, 21, 22, 23, 26, 27, 29, 30, 31, 32, 33, 35, 37, 38, 40, 44, 45, and 46. The first layer is described as the lateritic top soil, the second layer is made up of clay, the third layer which is the aquiferous unit is made up of sandstone, sandy clay or clayey sand. The VES points having five geo-electric layers include; VES 3, 6, 7, 8, 10, 11, 13, 15, 16, 17, 18, 19, 20, 24, 25, 28, 34, 36, 39, 41, 42, and 43. The layers are composed of lateritic top soil, clay/clayey sand, sandy clay/clay, sandstone/sandy clay/clay and clay in that order. The fourth layer represents the aquiferous unit.

Table 1: Summary Interpreted Geo-Electrical Layer Result Obtained from the Plotted Graphs

VES No.	Coordinates	Resistivity (Ωm)	Thickness (m)	Depth (m)	Transmissivity (m ² /day)	Inferred Lithology
VES 1	N7°43'19.21'' E8°26'33.64''	338.3	0.4	0.4	28.4589	Lateritic top soil
		10.2	4.1	4.5		clay
		178.9	9.3	13.8		sandstone
		2013.2				clay
VES 2	N7°43'33.54'' E8°26'11.80''	149.8	1.0	1.0	38.3279	Lateritic top soil
		9.7	2.2	3.1		clay
		212.4	14.7	17.9		sandstone
		28.5				clay
VES 3	N7°43'46.49'' E8°25'52.10''	471.5	0.6	0.6	64.8501	Lateritic top soil
		20.5	5.9	6.5		clay
		157.5	22.6	29.1		sandstone
		92.9	11.5	40.6		sandy clay
VES 4	N7°43'59.43'' E8°25'32.39''	362.2			114.3283	clay
		101.6	3.9	3.9		Lateritic top soil
		8.4	4.7	8.6		clay
		126.8	27.1	35.7		sandstone
VES 5	N7°44'12.37'' E8°25'12.69''	67.2			16.3464	sandy clay
		203.9	1.0	1.0		Lateritic top soil
		8.6	2.7	3.7		clay
		479.5	13.4	17.1		sandstone/siltstone
VES 6	N7°44'25.31'' E8°24'52.98''	16.5			35.2627	clay
		70.2	6.1	6.1		Lateritic top soil
		7.6	8.8	14.9		clay
		276.3	18.7	33.5		sandstone
VES 7	N7°44'38.26'' E8°24'33.27''	122.6	8.1	41.6	146.4736	sandy clay
		624.9				clay
		4327.0	0.3	0.3		Lateritic top soil
		57.8	12.1	12.4		sandstone
VES 8	N7°44'51.19'' E8°24'13.57''	11.5	13.8	26.2	1027.883	clay
		44.6	13.1	39.3		clayey sand
		251.5				sandstone
		314.0	0.7	0.7		Lateritic top soil
VES 9	N7°44'56.99'' E8°24'11.05''	16.4	2.4	3.1	14.3841	clay
		645.3	9.3	12.4		clayey sand
		12.9	53.9	66.3		clay
		36.6				clay
VES 10	N7°45'26.78'' E8°24'17.12''	699.7	0.5	0.5	698.7736	Lateritic top soil
		30.0	6.5	7.0		clay
		523.6	12.8	19.8		sandstone/siltstone
		15.8				clay
VES 11	N7°45'10.85'' E8°24'26.54''	187.0	3.3	3.3	79.3767	Lateritic top soil
		63.6	6.3	9.6		clay
		342.7	15.8	25.4		sandstone
		19.8	49.3	74.6		clayey sand
VES 12	N7°45'10.24'' E8°24'27.48''	43.9			85.4760	clay
		27.1	4.3	4.3		Lateritic top soil
		97.1	6.4	10.8		sandstone
		22.8	17.4	28.2		clay
VES 13	N7°45'00.72'' E8°24'41.97''	120.2	17.9	46.1	473.5496	sandy clay
		376.8				clay
		33.5	6.0	6.0		lateritic top soil
		326.7	7.0	13.0		sandstone
VES 14	N7°44'57.91'' E8°24'46.25''	78.8	13.0	26.0	68.9861	sandy clay
		23.3				clay
		45.3	9.0	9.0		Lateritic top soil
		170.7	13.8	22.9		sandstone
VES 15	N7°44'47.78'' E8°25'01.68''	27.6	10.9	33.7	674.9441	clay
		33.8	42.7	76.5		sandy clay
		39.2				clay
		36.9	1.0	1.0		Lateritic top soil
VES 16	N7°44'44.97'' E8°25'05.96''	78.9	10.2	11.2	69.3761	sandy clay
		165.8	21.0	32.1		sandstone
		26.1				clay
		42.9	1.6	1.6		Lateritic top soil
VES 16	N7°44'44.97'' E8°25'05.96''	48.2	9.1	10.6	69.3761	clay
		132.9	15.2	25.8		sandstone
		20.4	29.1	54.9		clay
		64.6				sandy clay
VES 16	N7°44'44.97'' E8°25'05.96''	46.9	1.6	1.6	69.3761	Lateritic top soil
		88.7	27.7	29.3		sandstone
		381.4	36.1	65.3		clay

Geophysical Characterization Of The Lithology And Aquifer Recharge Dynamic Of Lbrbda, ..

		147.2	18.9	84.2		sandy clay
		314.6				sandstone
VES 17	N7°44'34.84''	53.1	2.0	2.0	288.4594	Lateritic top soil
	E8°25'21.39''	140.0	5.2	7.2		sandstone
		94.5	22.6	29.8		clay
		29.6	17.6	47.4		sandy clay
		14.2				clay
VES 18	N7°44'32.03''	101.4	0.6	0.6	325.5522	Lateritic top soil
	E8°25'25.66''	22.9	1.7	2.3		sandstone
		542.7	14.2	16.5		clay
		52.5	33.9	50.4		sandy clay
		176.9				sandstone
VES 19	N7°44'21.89''	32.2	5.2	5.2	126.6246	Lateritic top soil
	E8°25'41.09''	322.5	11.2	16.4		sandstone
		23.4	33.2	49.6		clay
		64.6	16.0	65.5		sandy clay
		33.8				clay
VES 20	N7°44'19.09''	54.2	1.4	1.4	111.2768	Lateritic top soil
	E8°25'45.37''	12.3	2.6	4.0		clay
		95.3	16.2	20.2		sandstone
		73.7	15.9	36.1		sandy clay
		716.8				clay
VES 21	N7°44'08.95''	33.0	2.1	2.1	65.4364	Lateritic top soil
	E8°26'00.80''	16.2	4.7	6.8		clay
		309.9	35.7	42.5		sandstone
		235.4				sandy clay
VES 22	N7°44'06.14''	8.2	0.6	0.6	820.4230	Lateritic top soil
	E8°26'05.07''	389.0	4.6	5.2		sandstone
		13.4	23.9	29.1		clay
		158.7				sandy clay
VES 23	N7°43'56.01''	80.5	4.1	4.1	139.9352	Lateritic top soil
	E8°26'20.50''	175.5	7.9	12.1		sandy clay
		102.1	27.1	39.2		sandstone
		254.7				sandy clay
VES 24	N7°43'53.20''	23.2	2.5	2.5	105.8500	Lateritic top soil
	E8°26'24.78''	8.6	2.7	5.2		clay
		487.9	20.1	25.3		sandy clay
		147.0	28.8	54.1		sandstone
		102.1				sandy clay
VES 25	N7°43'42.35''	50.3	3.3	3.3	106.5730	Lateritic top soil
	E8°26'00.80''	422.9	7.0	10.2		clay
		40.0	30.0	40.3		sandy clay
		96.6	19.6	59.8		sandstone
		119.9				sandy clay
VES 26	N7°44'04.12''	90.5	1.2	1.2	80.8541	Lateritic top soil
	E8°26'51.05''	21.5	5.8	6.9		clay
		162.1	24.2	31.2		sandstone
		30.4				clay
VES 27	N7°44'15.66''	24.6	1.1	1.1	795.6949	Lateritic top soil
	E8°26'33.48''	288.5	24.8	25.9		sandstone
		18.3	61.0	86.9		clay
		56.7				sandy clay
VES 28	N7°44'18.47''	43.6	4.8	4.8	141.9913	Lateritic top soil
	E8°26'29.20''	238.6	7.2	11.9		sandy clay
		48.9	21.9	33.9		clay
		84.7	23.1	57.0		sandy clay
		235.5				sandstone
VES 29	N7°44'28.60''	120.4	1.3	1.3	81.8088	Lateritic top soil
	E8°26'13.77''	777.0	3.2	4.6		clay
		184.4	27.5	32.0		sandstone
		33.1				clay
VES 30	N7°44'31.41''	146.2	1.9	1.9	105.2571	Lateritic top soil
	E8°26'09.50''	2325.7	5.5	7.4		clay
		129.8	25.5	32.9		sandstone
		329.1				sandy clay
VES 31	N7°44'41.55''	7.3	0.4	0.4	44.3363	Lateritic top soil
	E8°25'54.07''	225.4	9.7	10.1		clay
		161.9	13.2	23.3		sandy clay
		4880.4				clay
VES 32	N7°44'52.44''	147.8	1.0	1.0	191.3294	Lateritic top soil
	E8°25'37.49''	1901.9	5.1	6.1		clay
		68.4	25.5	31.6		sandy clay
		703.6				clay
VES 33	N7°44'54.49''	324.2	0.5	0.5	13.6874	Lateritic top soil

Geophysical Characterization Of The Lithology And Aquifer Recharge Dynamic Of Lbrbda, ..

	E8°25'34.36"	21.8	1.9	2.4		clay
		598.6	13.8	16.2		clayey sand
		43.4				clay
VES 34	N7°45'07.43"	61.9	2.1	2.1	171.6870	Lateritic top soil
	E8°25'14.66"	1647.1	4.1	6.2		clay
		151.6	6.5	12.7		sandstone
		64.3	21.6	34.4		sandy clay
		419.3				clay
VES 35	N7°45'20.38"	72.1	2.8	2.8	37.8707	Lateritic top soil
	E8°24'54.95"	2353.8	6.3	9.2		clay
		150.0	10.5	19.7		sandy clay
		29.3				clay
VES 36	N7°45'26.58"	1336.7	0.5	0.5	13.7331	Lateritic top soil
	E8°24'59.05"	407.6	13.8	14.3		clay
		104.7	13.1	27.4		sandy clay
		472.3	11.1	38.5		sandstone/siltstone
		3603.7				clay
VES 37	N7°45'36.73"	385.0	1.1	1.1	9.8052	Lateritic top soil
	E8°24'43.58"	55.7	3.9	5.0		clay
		679.4	11.4	16.4		sandstone/siltstone
		13.8				clay
VES 38	N7°45'38.66"	1278.4	0.4	0.4	76.1840	Lateritic top soil
	E8°24'44.75"	431.7	32.0	32.4		clay
		121.1	17.3	49.8		sandy clay
		41.0				clay
VES 39	N7°45'23.06"	138.2	0.7	0.7	36.4396	Lateritic top soil
	E8°25'25.81"	1166.6	5.6	6.4		clay
		492.0	24.6	31.0		clayey sand
		389.4	24.6	55.6		sandstone
		161.1				clay
VES 40	N7°45'13.67"	40.1	0.5	0.5	15.2278	Lateritic top soil
	E8°25'49.77"	6873.2	6.2	6.7		clay
		321.6	8.6	15.3		sandstone
		28.3				clay
VES 41	N7°45'06.18"	301.3	7.4	7.4	26.7415	Lateritic top soil
	E8°26'09.97"	1481.9	11.8	19.2		clay
		32.1	47.2	66.4		sandy clay
		282.9	13.4	79.8		sandstone
		93.9				clay
VES 42	N7°44'57.13"	692.6	5.5	5.5	26.5462	Lateritic top soil
	E8°26'25.64"	798.1	11.6	17.1		clay
		207.3	22.8	39.9		sandy clay
		402.9	18.5	58.5		sandstone
		1239.1				clay
VES 43	N7°44'51.07"	2519.9	0.6	0.6	76.7652	Lateritic top soil
	E8°26'22.47"	390.6	4.2	4.8		sandstone
		818.9	11.3	16.1		clay
		190.5	26.6	42.7		sandstone
		1208.4				clay
VES 44	N7°44'38.13"	375.2	2.1	2.1	187.0574	Lateritic top soil
	E8°26'42.18"	3018.9	7.3	9.4		clay
		74.8	27.1	36.6		sandy clay
		458.1				clay
VES 45	N7°44'26.59"	99.9	0.7	0.7	130.4499	Lateritic top soil
	E8°26'59.75"	1383.5	4.4	5.1		clay
		153.7	47.0	52.1		sandy clay
		382.5				sandstone
VES 46	N7°44'39.80"	32.9	0.5	0.5	118.5576	Lateritic top soil
	E8°27'04.87"	1501.9	3.5	4.0		clay
		85.7	19.5	23.5		sandy clay
		728.2				clay

Figure 2 is the resistivity distribution map of the farm project. From the map the farm stretch increasing latitude toward the north and increasing longitude toward the East. Only two VES point were significantly high in resistivity and are aligned to the North while lower resistivity points were aligned to the south.

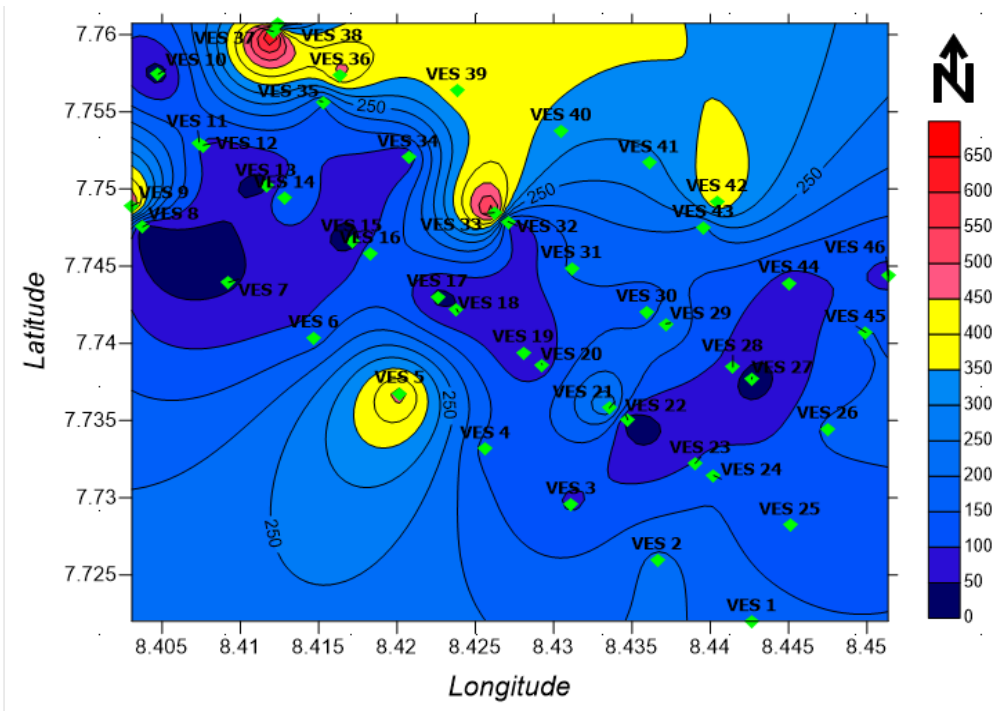


Figure 2: Showing the Resistivity Distribution Map of the Study Area

Figure 3 is the aquifer thickness map of the farm. Four VES locations recorded high thickness of between 65-90 cm and are positioned within the north east and north west region. Medium (35-64cm) and low (0-34cm) thickness dominate the entire field in all the quadrants of the study area.

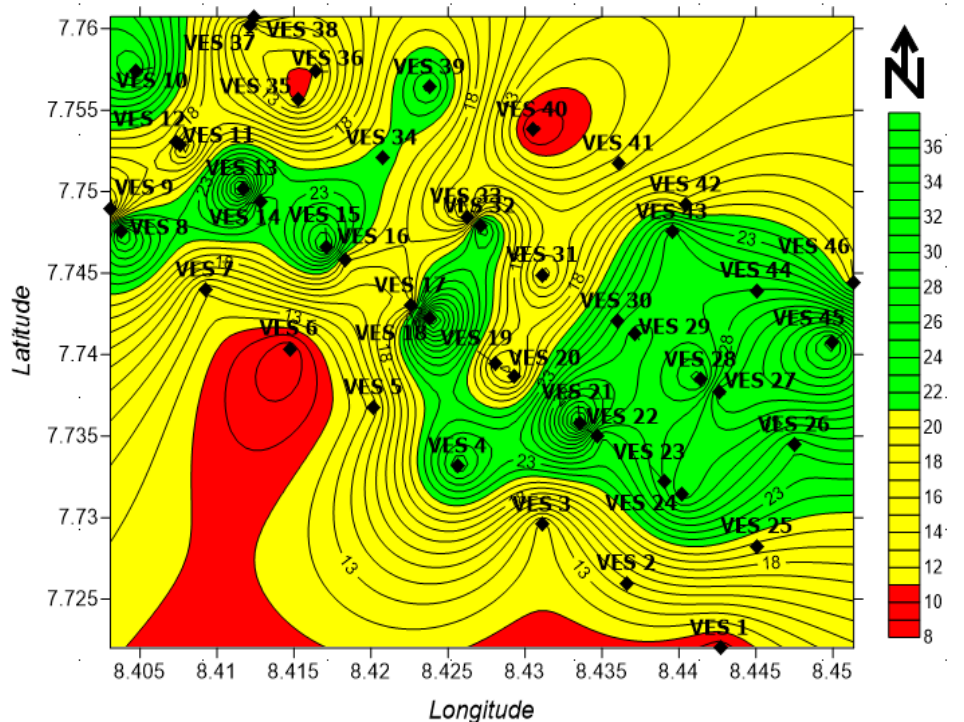


Figure 3: Aquifer Thickness Map of the Study Area

Figure 4 demonstrate the the Depth Distribution Map of the Study Area. The map classified the depth of aquifer into low, medium and high. The medium depth Ves locations were uniformly distributed across the study area with localised high depth aquifers in Ves 10, 16, 27 and 41. Low profile depth dominate the southern parts of the study area (Ves 1,2,4,and 5). The transmissivity in Figure 5 were between 650-950 and 150- 600

across the central region. While high transmissivity were recorded in the northern and southern parts of the farm, the centre regeion recorded medium to low transmissivity that stretches to the North west and South west.

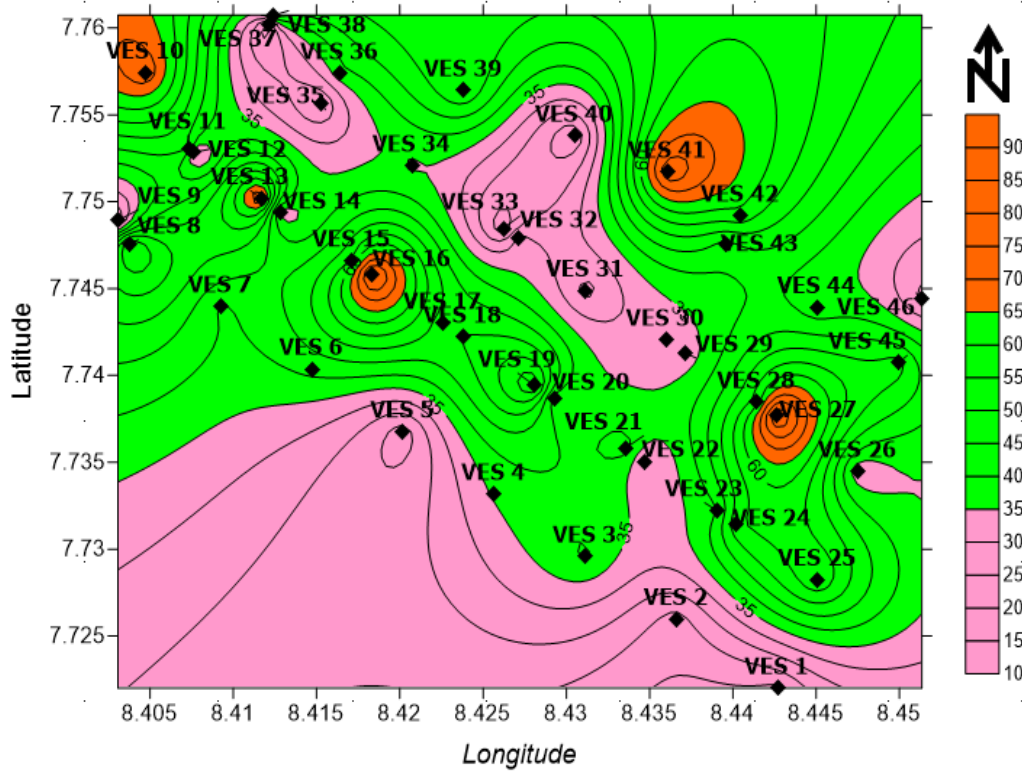


Figure 4: Showing the Depth Distribution Map of the Study Area

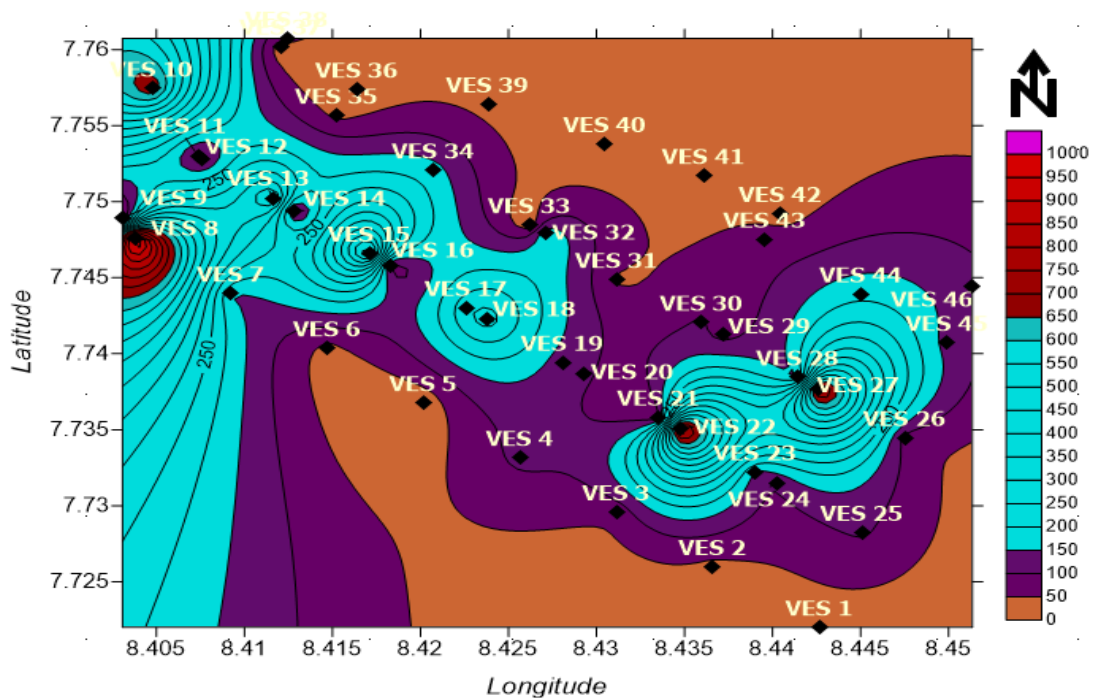


Figure 5: Showing the Transmissivity Distribution Map of the Study Area

III. DISCUSSION

3.1 Characteristic of lithology

Key important parameter in groundwater exploration are hydraulic conductivity and transmissivity; they are indices for understanding groundwater exploration properties and management as reported by (Ebong *et*

al., 2014; Hasan *et al.*, 2020; Huang *et al.*, 2011). Therefore, these two properties are essential in the interpretation of the data to identified aquifer layers at various sounding points showing the variation of aquifer resistivity and thickness due to lithologic composition, from which the longitudinal conductance, hydraulic conductivity and transmissivity were computed in accordance with (Eluozo *et al.*, 2012; Schwartz and Zang, 2003). . The aquifer resistivity in the study area ranges from 10 to 702 Ωm with an average value of 190.4 Ωm . From the results obtained, aquifer thickness ranges from 12.9 to 697.4 m having an average value of 175.8 m. The high thickness values at some VES points makes it prolific and desirable. The VES with the greatest thickness of 697.4 m was observed at VES 37 layout. The average theoretical value of hydraulic conductivity given by Niwas and Singhal (1981) is 8.64 m/day for pure sand and gravel hence average value from this study falls below this value, indicating that the study area is fraught with argillaceous bands of clay which is in agreement with the findings of Obiora and Ibuot.(2015)

Transmissivity values and its variation within the geologic formation was calculated and interpreted for classification of well potential. The primary distinction lies in the fact that transmissivity is the measure that extends over the vertical thickness of aquifer layer (Eluozo and Nwofor, 2012). The transmissivity values range from 35.56 to 1027.88 m^2/day , the average value been 159.51 m^2/day . The areas with high transmissivity can be attributed to having thick aquifer sand. The aquifer in the study area can be delineated as unconfined since it has non-porous layers above and below the aquifer zone. From the results of geoelectric parameters, the 3D contour maps were drawn to show the variation of the geoelectric parameters. From Figure 2 the contour map showing the distribution of aquifer resistivity as it decreases from east to west. This suggests that zones with low resistivity values will have high conductive geomaterials, as such poor groundwater quality. Figure 52 shows the distribution of aquifer thickness across the study area. It is observed that the eastern part of the study area have low aquifer thickness which extends northwards and can also be observed in parts of the western zone, thus indicating that thickness is not a major determining factor for resistivity.

3.2 Electrical layers

Vertical electrical sounding Geo-survey points results usually come out with geo-electric layers. In this study, four and five electrical layers were recorded. From Table 1, it can be seen that the vertical electrical sounding points having four geo-electric layers include; VES 1, 2, 4, 5, 9, 12, 14, 21, 22, 23, 26, 27, 29, 30, 31, 32, 33, 35, 37, 38, 40, 44, 45, and 46. The first layer is described as the lateritic top soil, the second layer is made up of clay, the third layer which is the aquiferous unit is made up of sandstone, sandy clay or clayey sand. However, places with aquiferous unit made up of sandstone and sandy clay have better groundwater potential. The vertical electrical sounding point having five geo-electric layers include; VES 3, 6, 7, 8, 10, 11, 13, 15, 16, 17, 18, 19, 20, 24, 25, 28, 34, 36, 39, 41, 42, and 43. The layers are composed of lateritic top soil, clay/clayey sand, sandy clay/clay, sandstone/sandy clay/clay and clay in that order. The fourth layer represents the aquiferous unit. The first layer has resistivity and thickness value ranges from 7.3 Ωm to 4327.0 Ωm and 0.3 m to 9.0 m respectfully. The wide range of the resistivity of the first layer is an indication of wide range in the composition of clay content in the lateritic soil. The second layer has resistivity ranges from 7.6 Ωm to 6873.2 Ωm with a thickness of 2.2m to 32.0 m. The third layer has resistivity range from 11.5 Ωm to 818.9 Ωm having a thickness of 8.6 m to 36.1m. The fourth layer has resistivity range from 12.9 Ωm to 4880.4 Ωm with thickness range from 8.1m to 53.9 m. The fifth layer has resistivity range from 14.2 Ωm to 3603.7 Ωm ; this layer has no defined thickness.

IV. CONCLUSSION AND RECOMMENDATION

4.1 Conclusion

In conclusion, the water table layer or zone within the study area is characterised with Sandy clay and sandstone formation which can serve as good layer for drilling sustainable tube wells for irrigation. Depth to water table is characterized as low water table spotting along the diagonal axis, therefore, care must be taken when selecting points for drilling tube wells along that area. The groundwater is classified into, poor, moderate, and good, with the extreme Northern part of the area characterized as poor and the remaining area having moderate to good groundwater potential. The aquifers thickness indicated that the aquifers within the study area have appreciable thickness suitable for tubewell however, few locations (VES 1, 6, 35, 36, and 40) have low aquifer thickness. The transmissivity test classified the groundwater potential into low, intermediate, high, and very high prospective. Low to moderate hydraulic conductivity indicating aquiferous zones which are permeable and capable of yielding appreciable groundwater for irrigation farming were recorded. It is therefore recommended that Tubewell development for irrigation farming within the study area should be concentrated in areas with moderate to good groundwater potential.

REFERENCE

- [1]. Anomohanran, O. (2013) Investigating the Geoelectric Response of Water Saturated and Hydrocarbon Impacted Sand in the Vicinity of Petroleum Pipeline. *International Journal of Applied Science and Technology*, 3, 14-21.
- [2]. Clarke, R. T.; Tucci, C. E.; Collischonn, W. (2003) Variabilidade temporal no regime hidrológico da bacia do rio Paraguai. *Revista Brasileira de Recursos Hídricos*. 8 (1), 201-211.
- [3]. Petts G. and Foster I. (1990) *Rivers and Landscape*. The Athenaeum Press, 3rd ed. New Castle, Great Britain.
- [4]. Silva Júnior, O. B.; Bueno, E. O.; Tucci, C. E. M.; Castro, M. N. R. (2003) Extrapolação Espacial na Regionalização da Vazão. *Revista Brasileira de Recursos Hídricos*. 8(1), 21–37.
- [5]. Tucci C.E.M (2002) Regionalização de vazões. (Regionalization of flow rates). Ed. Universidade/UFRGS, p 256.
- [6]. Ityavyar J. A., Inah E. I., Akosim C. (2011) Assessment of Captive Management of Nile Crocodile, *Crocodylus Niloticus*, In three towns of Benue State, Nigeria. *Journal of Research In Forestry, Wildlife And Environment*. Volume 3 No. 2, 12-23.
- [7]. Obiora D. N., Ibuoti J. C., George N. J. (2016). Evaluation of aquifer potential, geoelectric and hydraulic parameters in Ezza North, southeastern Nigeria, using geoelectric Sounding. *Int J Environ Sci. Technol.*, 13:435–444.
- [8]. Clark, L. (1985) Groundwater Abstraction from Basement Complex Area of Africa. *Quarterly Journal of Engineering Geology and Hydrogeology*, 18, 25-34. <https://doi.org/10.1144/GSL.QJEG.1985.018.01.05>
- [9]. Amiri V, Sohrabi N, Li P, Shukla S. Estimation of hydraulic conductivity and porosity of a heterogeneous porous aquifer by combining transition probability geostatistical simulation, geophysical survey, and pumping test data. *Environ Dev Sustain*. 2023;25(8):7713–36.
- [10]. Omosuyi, G.O. and Oseghale, A. (2012) Groundwater Vulnerability Assessment in I. A. Adeyemo et al.251 Shallow Aquifers Using Geoelectric and Hydrogeologic Parameters at Odigbo, Southwestern Nigeria. *Journal of Scientific and Industrial Research*, 3, 501-512.
- [11]. Abiola, O., Enikanselu, P.A. and Oladapo, M.I. (2009) Groundwater Potential and Aquifer Protective Capacity of Overburden Units in Ado-Ekiti, Southwestern Nigeria. *International Journal of Physical Sciences*, 4, 120-132.
- [12]. Adeyemo, I.A., Omosuyi, G.O., Olayanju, G.M. and Omoniyi, G.K. (2014) Hydro-geologic and Geoelectric Determination of Groundwater Flow Pattern in Alaba-Apatapiti Layouts, Akure, Nigeria. *The International Journal of Engineering and Science (IJES)*, 3, 44-52.
- [13]. Amadi, A.N., Nwawulu, C.D., Unuevho, C.I. and Ako, T.A. (2011) Evaluation of the Groundwater Potential in Pompo Village, Gidan Kwano, Minna Using Vertical Electrical Resistivity Sounding. *British Journal of Applied Science & Technology*, 1, 53-66. <https://doi.org/10.9734/BJAST/2011/192>
- [14]. Kosinski, W.K. and Kelly, W.E. (1981) Geoelectric Soundings for Predicting Aquifer Properties. *Groundwater*, 19, 163-171. <https://doi.org/10.1111/j.1745-6584.1981.tb03455.x>
- [15]. Mogaji, K.A., Omosuyi, G.O. and Olayanju, G.M. (2011) Groundwater System Evaluation and Protective Capacity of Overburden Material at Ile-Oluji, Southwest-ern Nigeria. *Journal of Geology and Mining Research*, 3, 294-304.
- [16]. Olayanju, G.M., Ayuk, M.A. and Adelusi, A.O. (2011) Geotechnical Mapping of the Groundwater Regime around the Federal Polytechnic, Ado-Ekiti, Southwestern Nigeria. *Journal of Geology and Mining Research*, 3, 201-210
- [17]. Akhter G, Hasan MJ. Determination of aquifer parameters using geoelectrical sounding and pumping test data in Khanewal District Pakistan. *Open Geosci*. 2016;8(1):630–8.
- [18]. Akintorinwa OJ, Okoro OV. Combine electrical resistivity method and multi-criteria GIS-based modeling for landfill site selection in the Southwestern Nigeria. *Environ Earth Sci*. 2019;78:1–6.
- [19]. Anomohanran O. Hydrogeophysical investigation of aquifer properties and lithological strata in Abraka Nigeria. *J Afr Earth Sci*. 2015;1(102):247–53.
- [20]. Ebong ED, Akpan AE, Onwuegbuche AA. Estimation of geohydraulic parameters from fractured shales and sandstone aquifers of Abi (Nigeria) using electrical resistivity and hydrogeologic measurements. *J Afr Earth Sc*. 2014;1(96):99–109.
- [21]. Eluozo SN, Nwofor TC. Evaluating the variation of transmissivity on groundwater development in Rivers State. *Int J Appl Environ Sci*. 2012;7(2):141–7.
- [22]. Erram VC, Gupta G, Pawar JB, Kumar S, Pawar NJ. Potential groundwater zones in parts of Dhule District, Maharashtra: a joint interpretation based on resistivity and magnetic data. *J India Geol Congr*. 2010;2(1):37–45.
- [23]. Hasan M, Shang Y, Akhter G, Jin W. Delineation of contaminated aquifers using integrated geophysical methods in Northeast Punjab Pakistan. *Environ Monit Assess*. 2020;192:1–5.
- [24]. Hasan M, Shang Y, Akhter G, Jin W. Geophysical assessment of groundwater potential: a case study from Mian Channu Area Pakistan. *Groundwater*. 2018;56(5):783–96.
- [25]. Huang YP, Kung WJ, Lee CH. Estimating aquifer transmissivity in a basin based on stream hydrograph records using an analytical approach. *Environ Earth Sci*. 2011;63:461–8.
- [26]. Manu E, Agyekum WA, Duah AA, Tagoe R, Preko K. Application of vertical electrical sounding for groundwater exploration of Cape coast municipality in the central region of Ghana. *Arab J Geosci*. 2019;12:1–1.
- [27]. Mehmood Q, Mahmood W, Awais M, Rashid H, Rizwan M, Anjum L, Muneer MA, Niaz Y, Hamid S. Optimizing groundwater quality exploration for irrigation water wells using geophysical technique in semi-arid irrigated area of Pakistan. *Groundw Sustain Dev*. 2020;1(11):100397.
- [28]. Mohammed MA, Szabó NP, Szűcs P. Exploring hydrogeological parameters by integration of geophysical and hydrogeological methods in northern Khartoum state, Sudan. *Groundw Sustain Dev*. 2023;1(20):100891.
- [29]. Niwas S, Gupta PK, de Lima OA. Nonlinear electrical response of saturated shaley sand reservoir and its asymptotic approximations. *Geophysics*. 2006;71(3):G129–
- [30]. Nwachukwu S, Bello R, Balogun AO. Evaluation of groundwater potentials of Orogun, South-South part of Nigeria using electrical resistivity method. *Appl Water Sci*. 2019;9(8):184.
- [31]. Oldenborger GA, Knoll MD, Routh PS, LaBrecque DJ. Time-lapse ERT monitoring of an injection/withdrawal experiment in a shallow unconfined aquifer. *Geophysics*. 2007;72(4):F177–87.
- [32]. Oli IC, Opara AI, Okeke OC, Akaolisa CZ, Akakuru OC, Osi-Okeke I, Udeh HM. Evaluation of aquifer hydraulic conductivity and transmissivity of Ezza/Ikwo area, Southeastern Nigeria, using pumping test and surficial resistivity techniques. *Environ Monit Assess*. 2022;194(10):719.
- [33]. Oyeyemi KD, Aizebeokhai AP, Metwaly M, Oladunjoye MA, Bayo-Solarin BA, Sanuade OA, Thompson CE, Ajayi FS, Ekhaguere OA. Evaluating the groundwater potential of coastal aquifer using geoelectrical resistivity survey and porosity estimation: a case in Ota, SW Nigeria. *Groundw Sustain Dev*. 2021;1(12):100488.
- [34]. Schwartz WF, Zang H. *Fundamentals of Groundwater*. Hoboken: John Walley & Sons Inc; 2003. p. 50–5.

- [35]. Shah SH, Jianguo Y, Jahangir Z, Tariq A, Aslam B. Integrated geophysical technique for groundwater salinity delineation, an approach to agriculture sustainability for Nankana Sahib Area, Pakistan. *Geomat Nat Haz Risk*. 2022;13(1):1043–64.
- [36]. Sikandar P, Bakhsh A, Arshad M, Rana T. The use of vertical electrical sounding resistivity method for the location of low salinity groundwater for irrigation in Chaj and Rachna Doabs. *Environ Earth Sci*. 2010;60:1113–29.
- [37]. Subba RN. Groundwater prospecting and management in an agro-based rural environment of crystalline terrain of India. *Environ Geol*. 2003;43:419–31.
- [38]. Taha AI, Al Deep M, Mohamed A. Investigation of groundwater occurrence using gravity and electrical resistivity methods: a case study from Wadi Sar, Hijaz Mountains Saudi Arabia. *Arab J Geosci*. 2021;14:1.
- [39]. Umoh JA, George NJ, Ekanem AM, Emah JB. Characterization of hydro-sand beds and their hydraulic flow units by integrating surface measurements and ground truth data in parts of the shorefront of Akwa Ibom State, Southern Nigeria. *Int J Energy Water Resour*. 2022;21:1–7.
- [40]. Wahab S, Saibi H, Mizunaga H. Groundwater aquifer detection using the electrical resistivity method at Ito Campus, Kyushu University (Fukuoka, Japan). *Geosci Lett*. 2021;8:1–8.